REPORT DOCUMENTATION PAGE

Form Approved
OMB No. 0704-0188

1. AGENCY USE ONLY (Leave blank)	2. REPORT DATE	3. REPORT TYPE AND DATES COVERED
	11/20/96	Final 9/1/93 - 8/31/96

4. TITLE AND SUBTITLE
Investigation of Novel Quantum Well Structures for Non-linear Optics

5. FUNDING NUMBERS
N00014-93-1-1061

6. AUTHOR(S)
J. S. Harris

7. PERFORMING ORGANIZATION NAME(S) AND ADDRESS(ES)
Stanford University
329 CISX
Solid State Electronics Lab
Stanford, CA 94305-4075

8. PERFORMING ORGANIZATION REPORT NUMBER

9. SPONSORING/MONITORING AGENCY NAME(S) AND ADDRESS(ES)
Office of Naval Research Regional Office Seattle
1107 NE 45th Street, Suite 350
Seattle, WA 98105-4631

10. SPONSORING/MONITORING AGENCY REPORT NUMBER

11. SUPPLEMENTARY NOTES

12a. DISTRIBUTION/AVAILABILITY STATEMENT

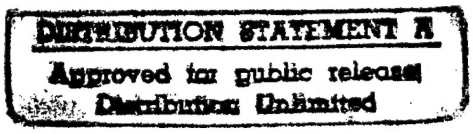

12b. DISTRIBUTION CODE

13. ABSTRACT *(Maximum 200 words)*

See attached

14. SUBJECT TERMS

15. NUMBER OF PAGES

16. PRICE CODE

17. SECURITY CLASSIFICATION OF REPORT	18. SECURITY CLASSIFICATION OF THIS PAGE	19. SECURITY CLASSIFICATION OF ABSTRACT	20. LIMITATION OF ABSTRACT
Unclassified	unclassified	Unclassified	Unclassified

SOLID STATE ELECTRONICS LABORATORY

DEPARTMENT OF ELECTRICAL ENGINEERING
STANFORD UNIVERSITY · STANFORD, CA 94305
TELEPHONE: FAX: 415-723-4659

November 26, 1996

Defense Technical Information Center
Building 5, Cameron Station
Alexandria, VA 22304-6145

Enclosed is a copy of the Final Report for AASERT Grant #N00014-93-1-1061 for the period 9/1/93-8/31/96.

Sincerely yours

J. S. Harris

J. S. Harris
Director Solid State Laboratory
Professor Electrical Engineering

FINAL REPORT

Contract N00014-93-I-1061

Investigation of Novel Quantum Well Structures for Non-Linear Optics

This is the final report for AASERT increment #N00014-93-I-1061 to contract N00014-92-J-1903. Intitially, Herman Chui was supported and upon completion of his Ph.D., Chris Ebert, was added to the CNOM project to develop a mid-infrared light source using form birefringent waveguides. A compact, integrated mid-infrared light source (~ 3-5 μm) would have several applications, including airborne countermeasures and spectroscopy. The efforts here are aimed at creating nonlinear wavegudies that can, through the process of Difference Frequency Generation (DFG), mix two near-infrared laser diodes and generate a long wavelength output.

One of the most interesting properties of "artificially structured" materials is that they can exhibit properties that are absent in the bulk materials of which they are composed. Such an example is the birefringence exhibited in multilayer stacks of materials, where the component materials are isotropic. This effect is known as form birefringence. Thus, waves traversing the medium with their electric fields perpendicular to the plane (TM) experience a different index of refraction than TE waves (those with electric field parallel to the plane). This difference is due to the different boundary conditions imposed on electric fields parallel and perpendicular to dielectric interfaces.

The GaAs/AlAs material system is an interesting candidate for creating these multilayer strucutres. The indices of refraction for these materials are well characterized, and mature growth techniques (MBE, MOCVD) exist to deposit sufficiently thin layers of optical quality material, and they are compatible for integration with semiconductor lasers.

The amount of birefringence attainable depends on the index difference between the two layers used. Since greater birefringence leads to phasematching conditions over a wider range of wavelengths, it is desirable to increase this ratio as much as possible. One viable technique is to use oxidized AlAs. This material is formed by etching down into epilayers containing AlAs. The sample is then placed in a furnace tube at around 450° C, with N_2 flowing through a bubbler of distilled water at 95.0° C. The steam then reacts with the AlAs, forming Al_2O_3 and AsH_3 as the result. Lateral distances on the order of 100 μm have been reported to be successfully oxidized. The

addition of a small percentage of Ga to the AlAs strongly decreases the oxidation rate, allowing different layers to be oxidized over different distances. The oxidized AlAs is an amorphous form of Al_2O_3, which is insulating and low-index (n ~ 1.5 - 1.6). Accordingly, the amount of birefringence that can be achieved is greately increased. This low index can also serve as a buffer layer, shielding the waveguide core from the high index GaAs susbtrate. Because the oxidation procedes laterally, multilayers structures can be oxidized, creating superlattices of crystalline and amorphous material. These superlattices can then be modeled as a birefringent material, with polarization-dependent indices of refraction.

This birefringence can be used to design a waveguide for nonlinear frequency conversion. One key to efficient frequency conversion is to phasematch the interaction. By engineering the birefringence of the waveguide materials, two different wavelengths can be made to propagate with the same effective index. Thus, power is continuously transferred from the pump frequency to the signal frequency, instead of building up in the signal frequency for a short distance and then transferring back to the pump. Because of the increased confinement and long interaction length of a waveguide structure, a very efficient device should result. The only nonzero nonlinear tensor element for GaAs and AlAs is $\chi^{(2)}_{xyz}$. Thus, two of the waves in the nonlinear interaction need to be polarized in the x-y plane, or TE direction, and one in the TM direction. Because $n_{TE} > n_{TM}$, it then becomes necessary to have the shorter wavelength TM polarized, in order to offset the natural dispersion of the material. In addition, it is desirable to use as high a duty cycle of GaAs as possible for two reasons. First, the higher duty cycle of GaAs results in a stronger nonlinear interaction, since $\chi^{(2)}$ of oxidized AlAs is negligible. Secondly, the phasematched effective mode indices are higher, so there will be less radiation loss into the GaAs substrate.

Current research involves growing, fabricating, and testing these waveguide structures. Present efforts are concentrating on microfabrication techniques for making low loss waveguides. This involves issues such as mask design and wet versus dry etching. In addition, the oxidation process is being studied in order to design structures to better utilized the unique capabilities of oxidized AlAs. Finally, testing procedures will be developed to measure both the linear (loss, birefringence) and nonlinear (conversion efficiency) of the waveguides.

Other alternatives for creating mid infra-red light have also been explored. One of these has been to use a patterned template for growing a quasiphasematched GaAs

waveguide. If the GaAs lattice can be rotated by 90°, then the sign of $\chi(2)$ changes. In order to take advantage of this fact, two wafers are first bonded together, but rotated with 90° with respect to one another. Then, through lapping and etching, the majority of one of the wafers is removed. A quasiphasematching grating is then patterned, leaving alternating regions of the rotated wafer on top of the original substrate. This template is then put into the MBE machine for regrowth, and the waveguide structure is grown as it would normally be. In regions were the bonded wafer is left on, $\chi(2)$ has one sign, whereas in the ares where it was removed the signs are opposite.

Publications and Ph.D. theses supported by AASERT

Ph.D. Thesis

"Mid-Infrared Light Generational by Non-Linear Optical Frequency Conversion in Interband in InGaAs/AlGaAs Quantum Wells," Herman Chui, Ph.D. Thesis, Stanford University, August 1994.

Publications

H. C. Chui, S. M. Lord, E. Martinet, M. M. Fejer and J. S. Harris, Jr., "Intersubband Transitions in High Indium Content InGaAs/AlGaAs Quantum Wells," *Appl. Phys. Lett.* **63** (3), pp. 364-366, July 1993. (appended)

H. C. Chui, E. L. Martinet, M. M. Fejer, and J. S. Harris, Jr., "Short Wavelength Intersubband Transitions in InGaAs/AlGaAs quantum wells grown on GaAs," *Appl. Phys. Lett.* **64** (6), pp. 736-738, February 1993.

H. C. Chui and J. S. Harris, Jr., "Growth Studies on $In_{0.5}Ga_{0.5}As$/AlGaAs Quantum Wells Grown on GaAs with a Linearly Graded InGaAs Buffer", *J. Vac. Sci. Technol. B* **12** (2), pp. 1019-1022, Mar/Apr 1994.

H. C. Chui, E. L. Martinet, M. M. Fejer, and J. S. Harris, Jr., "Large Energy Intersubband Transitions in High Indium Content InGaAs/AlGaAs Quantum Wells," NATO ASI: Quantum Well Intersubband Transition Physics and Devices, H. C. Liu, B. F. Levine, J. Y. Andersson, eds., Kluwer Academic Publishers, pp. 251-9 (1994).

H. C. Chui, E. L. Martinet, G. L. Woods, M. M. Fejer, and J. S. Harris, Jr., "Doubly resonant second harmonic generation of 2.0 μm light in coupled InGaAs/AlAs Quantum Wells", *Appl. Phys. Lett.* **64** (25), pp. 3365-3367, June 1994 (appended).

H. C. Chui, G. L. Woods, M.M. Fejer, E. L. Martinet, and J.S. Harris, Jr., "Tunable Mid-Infrared Generation by Difference Frequency Mixing of Diode Laser Wavelengths in Intersubband InGaAs/AlAs Quantum Wells," *Appl. Phys. Lett.* **66** (3), pp. 265-267, Janauary 1995 (appended).

L. A. Eyres, C. B. Ebert, H. C. Chui, J. S. Harris, Jr., and M. M. Fejer, "Fabrication of GaAs Orientation Template Substrates for Quasi-Phasematched Guided-Wave Nonlinear Optics," in *Nonlinear Guided Waves and Their Applications*, Vol. 6, 1995 OSA Technical Digest Series (Optical Society of America, Washington DC, 1995), pp. 156-158.

Doubly resonant second harmonic generation of 2.0 μm light in coupled InGaAs/AlAs quantum wells

H. C. Chui, E. L. Martinet, G. L. Woods, M. M. Fejer, and J. S. Harris, Jr.
Center for Nonlinear Optical Materials Research, McCullough 226, Stanford University, Stanford, California 94305-4055

C. A. Rella, B. I. Richman, and H. A. Schwettman
Stanford Picosecond FEL Center, W. W. Hansen Experimental Physics Laboratory, Stanford University, Stanford, California 94305-4085

(Received 2 February 1994; accepted for publication 20 April 1994)

We demonstrate intersubband absorption and second harmonic generation (SHG) in asymmetric coupled $In_{0.6}Ga_{0.4}As$/AlAs n-type quantum wells (QWs) grown on a GaAs substrate. Intersubband absorption at 4.1 and 2.1 μm wavelengths, corresponding to the 1 to 2 and 1 to 3 transitions, respectively, are observed. SHG of 2.0 μm light is demonstrated in this doubly resonant QW. This is the shortest wavelength SHG to date in any n-type QW system. The second order nonlinear susceptibility $\chi^{(2)}$ is measured using a free electron laser by interference of the second harmonic fields from the QW and substrate. At a pump wavelength of 4.0 μm, a large asymmetry in the SHG power with rotation angle of the sample arising from SHG from the QW is observed, and a $\chi^{(2)}$ of magnitude 20 ± 8 nm/V, approximately 100 times that of bulk GaAs, and phase $63°\pm34°$ relative to the GaAs substrate is measured. Comparison of both the linear and nonlinear properties to a simple model is discussed.

Quantum wells (QWs) have been demonstrated to have extremely large nonlinear susceptibilities arising from intersubband transitions.[1–4] These large nonlinear susceptibilities may result in efficient nonlinear optical frequency conversion and electro-optic switching devices.[5] These intersubband transitions are typically limited to the far and mid-infrared, but recent advances in strained QW materials have allowed intersubband transition energies in n-type QWs to reach the technologically important 2 μm wavelength,[6,7] where compact InGaAsP and GaSb diode laser sources[8] as well as diode pumped Tm:Ho:YAG lasers are available. However, the nonlinear optical properties from these short wavelength intersubband transitions have only begun to be investigated.[9] In this work, we report both intersubband absorption and second harmonic generation (SHG) of 2 μm light in asymmetric coupled InGaAs/AlAs QWs.

The asymmetric coupled QW structure used for these studies was designed to be doubly resonant for efficient SHG. The QW subband eigenstates were modeled with a single band effective mass model with nonparabolicity included using an energy-dependent effective mass as described previously.[7] Band bending was not taken into account. The coupled QW consisted of two heavily doped (sheet charge density of 3.0×10^{12} cm^{-2} per coupled QW) $In_{0.6}Ga_{0.7}As$ wells of 31.1 and 12.7 Å thicknesses separated by a 5.65 Å AlAs intermediate barrier. One monolayer of GaAs was added to either end of the double well to smooth the interfaces between the AlAs barrier and InGaAs wells.[10] The band diagram of the coupled quantum well with calculated subband energies and wave functions is shown in Fig. 1. The calculated intersubband transition energies and dipole moments are $E_{12}=297$ meV, $E_{13}=523$ meV, $z_{12}=9.7$ Å, $z_{13}=-6.0$ Å, $z_{22}-z_{11}=21.1$ Å, and $z_{23}=11.0$ Å. 200 periods of the coupled QWs separated by 100 Å AlAs barriers were grown on a (100) semi-insulating GaAs substrate by molecular beam epitaxy (MBE) in a Varian Gen II system. A linearly graded InGaAs buffer with a final indium composition of 30% was used to provide strain compensation in the QWs.[11,12] The sample was grown at a substrate temperature of 375 °C with As_4. Details of the growth studies used to optimize the growth conditions for $In_{0.5}Ga_{0.5}As$/AlGaAs QWs are given elsewhere.[10]

The intersubband absorption of the sample was measured using a Fourier transform infrared (FTIR) spectrometer with the sample mounted at Brewster's angle to the TM polarized light. The absorption spectrum of the sample is shown in Fig. 2. Absorption peaks at $E_{12}=300$ meV (4.1 μm) and $E_{13}=580$ meV (2.1 μm) are observed. To our knowledge, this is the largest E_{13} reported to date. These measured intersubband energies are within 10% of the theoretically predicted values. Lorentzian lineshapes fit to the absorption peaks yield half-width at half-maximum (HWHM) linewidths of $\Gamma_{12}=41$ meV and $\Gamma_{13}=67$ meV and integrated absorption fractions (IAFs) of 28.1 and 9.8 mAbs meV/QW for the 1 to 2 and 1 to 3 transitions, respectively. Assuming $z_{12}=9.7$ Å from theory, the measured IAFs

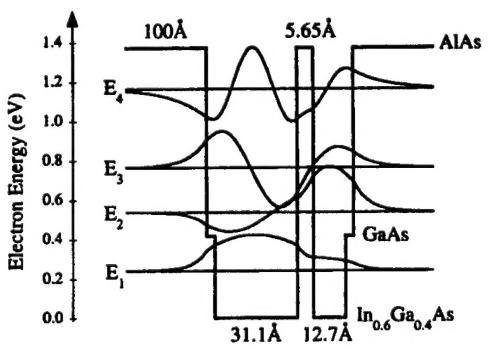

FIG. 1. Conduction band diagram of the asymmetric coupled QW with calculated subband energies and wave functions.

 0003-6951/94/64(25)/3365/3/$6.00

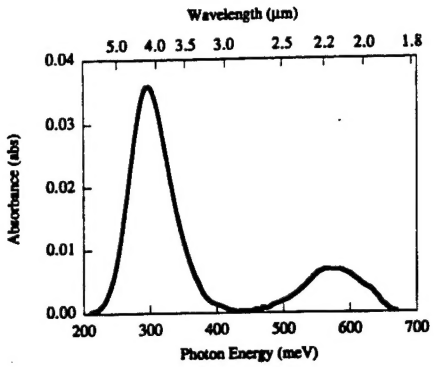

FIG. 2. Absorption spectrum of the coupled QW showing intersubband absorption peaks at 4.1 and 2.1 μm wavelengths corresponding to the 1 to 2 and 1 to 3 transitions, respectively.

yield an effective doping concentration $\sigma_{\text{eff}}=3.0\times10^{12}$ cm^{-2}/QW and $|z_{13}|=4.2$ Å.[13]

The second order nonlinear susceptibility $\chi^{(2)}$ of the QW, $\chi^{(2)}_{\text{QW}}$, can be calculated by treating the QW as a three-level system. If the ith subband to jth subband transition has a Lorentzian line shape with dipole moment z_{ij} and HWHM linewidths of Γ_{ij}, then near double resonance, $\chi^{(2)}$ is given by[14]

$$\chi^{(2)}_{\text{QW}}\cong\frac{2q^3N_{\text{eff}}}{\epsilon_0}\sum_{m,n}\frac{z_{1n}z_{nm}z_{m1}}{(\hbar\omega-E_{1n}-i\Gamma_{1n})(2\hbar\omega-E_{1m}-i\Gamma_{1m})}, \tag{1}$$

where only the ground state subband is assumed to be occupied with a carrier concentration, N_{eff}. This formulation neglects inhomogeneous broadening of the intersubband transitions as well as local field effects due to charge screening in the QW layers. Using the intersubband transition parameters derived from the intersubband absorption measurement, $N_{\text{eff}}=\sigma_{\text{eff}}/l_{\text{QW}}$, where $l_{\text{QW}}=155.1$ Å is the QW period, and assuming $z_{22}-z_{11}=21.1$ Å and $z_{23}=11.0$ Å from theory, an estimate for $\chi^{(2)}_{\text{QW}}$ is obtained. The calculated magnitude and phase of $\chi^{(2)}_{\text{QW}}$ is shown in Fig. 3. The double resonant peak of the $\chi^{(2)}_{\text{QW}}$ is near 4.5 μm wavelength with a magnitude of 12 nm/V.

SHG measurements were performed with a free electron laser (FEL) tuned to a wavelength of 4.0 μm. The Stanford FEL[15] generates pulses with pulse lengths of a few picoseconds, a peak power of several hundred kilowatts, and a linewidth of approximately 10 nm. The pump beam was focused onto the sample with a focal spot diameter of 100 μm. The QW and reference samples were placed in a rotation stage which allowed varying the incidence angle θ and rotating in angle ϕ about the sample normal. Multilayer dielectric filters were placed both before and after the sample in order to prevent incident 2.0 μm radiation from the FEL from reaching the sample and to block the 4.0 μm pump radiation from reaching the detector, respectively. The power leakage through the filters at the blocking wavelengths was determined to be below the detector noise level. ZnSe polarizers were used on both the input and collection side to select only the TM polarization. A PbS detector was used to measure the SHG signal. In addition, a portion of the FEL pump beam

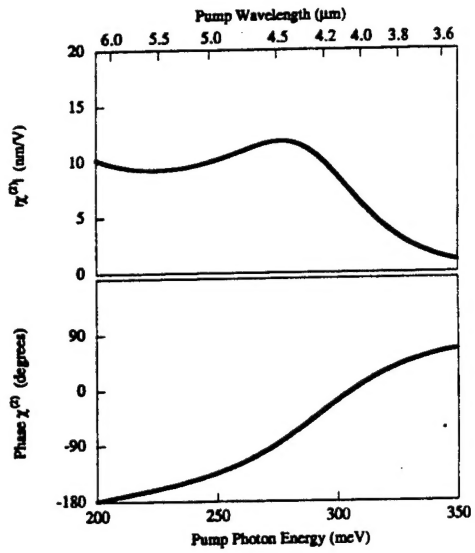

FIG. 3. Calculated spectrum of the magnitude (top graph) and phase (bottom graph) of SHG $\chi^{(2)}$ for the coupled QW.

was focused onto a properly phase matched $AgGaSe_2$ crystal and detected with an InSb detector for use as a reference SHG signal. The measured SHG power was then normalized to fluctuations in the pump power by dividing by the reference SHG signal.

$\chi^{(2)}_{\text{QW}}$ was measured by mixing the second harmonic (SH) from the QW with the SH from the GaAs substrate.[14] Since the symmetry of $\chi^{(2)}$ in bulk GaAs is different than that in QWs, polarization selection can be used to extract $\chi^{(2)}_{\text{QW}}$. The $\chi^{(2)}_{\text{QW}}$ tensor has a nonzero (zzz) element, and the $\chi^{(2)}_{\text{GaAs}}$ tensor has a nonzero (xyz) element. If only the TM polarization is selected, the SHG conversion at frequency ω from the QW sample is given by[9]

$$\frac{I_{2\omega}}{I_\omega^2}\propto\left|\chi^{(2)}_{\text{GaAs}}\cos2\phi\sin\zeta e^{i\zeta}+\frac{\pi l_{\text{MQW}}\sin^2\theta_{\text{int}}}{6l_c\cos^2\theta_{\text{int}}}\chi^{(2)}_{\text{QW}}\right|^2, \tag{2}$$

where $I_{2\omega}$ and I_ω are the SH and pump intensities, ϕ is the angle between the projection of the pump beam onto the sample and the (110) direction of the sample, θ is the incidence angle (angle between the sample normal and the pump beam) with internal angle θ_{int}, l_{MQW} is the total thickness of the MQW layers,

$$\zeta\cong\frac{\pi}{2}\frac{L}{l_c\cos\theta_{\text{int}}} \tag{3}$$

is half the phase mismatch between the pump and SH fields, L is the total thickness of the combined MQW and substrate, and

$$l_c=\frac{\pi c}{2\omega(n_{2\omega}-n_\omega)} \tag{4}$$

is the coherence length in GaAs. For our sample, $l_{\text{MQW}}=3.1$ μm and $L=401$ μm. Then, if l_c is known with sufficient accuracy, $\chi^{(2)}_{\text{QW}}$ can be extracted by measuring the SHG conversion efficiency versus angle ϕ and fitting to Eq. (2).

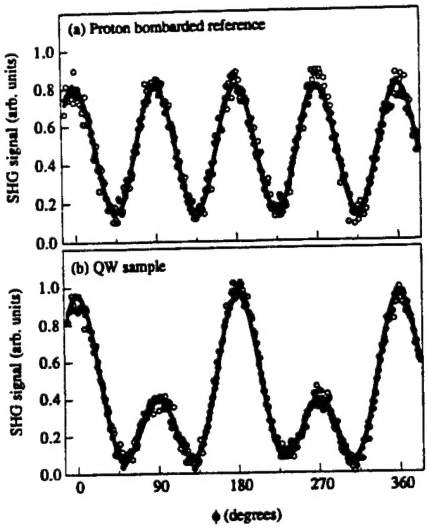

FIG. 4. Measured (hollow circles) and theoretically fitted (solid lines) normalized SHG power vs rotation angle ϕ for the proton bombarded reference (top graph) and QW sample (bottom graph) at a pump wavelength of 4.0 μm.

The value of l_c can be obtained via Eq. (4) by using published values of the refractive index of GaAs.[16] However, an accuracy of 10^{-3} for the indices of refraction yields an accuracy of only $\pm 10\%$ on l_c. By using a wedge technique,[14,17] we determined that the coherence length l_c is 44.7 ± 2.1 μm and 52.7 ± 1.8 μm at 4.8 and 5.19 μm wavelengths, respectively. The values of l_c calculated from the refractive index data lie within the error bars of these directly measured values. Thus, we have confidence in assuming that $l_c=28.86$ μm to an accuracy of $\pm 4\%$ at 4.0 μm as calculated from the refractive index data.

We measured the normalized SHG power versus angle ϕ for both the QW sample and a proton bombarded QW sample for reference (proton bombardment causes trapping of the conduction band electrons so that $\chi^{(2)}_{QW}$ is zero[3]). These ϕ scans were taken at $\theta=45°$ and are shown in Fig. 4. The proton bombardment reference has even peaks of 0°, 90°, 180°, and 270° arising, respectively, from alignment of the incident polarization to the (110), ($\bar{1}$10), ($\bar{1}\bar{1}$0), and (1$\bar{1}$0) crystal directions of the GaAs. As also shown in Fig. 4(a), this reference ϕ scan fits a $\cos^2(2\phi)$ dependence. The QW sample, on the other hand, has a large asymmetry in the ϕ scan with stronger 0° and 180° peaks than 90° and 270° peaks. This large asymmetry is due to addition of the ϕ-independent QW SH field to the ϕ-dependent substrate SH field, so that the resulting intensity follows a $(\cos 2\phi+\text{constant})^2$ dependence as given in Eq. (2). By fitting the QW ϕ scan to Eq. (2) with a complex $\chi^{(2)}_{QW}$ fitting parameter, while allowing for variations of $\pm 4\%$ in l_c and $\pm 5\%$ of the maximum signal as an offset of the signal due to uncertainty in the baseline of the SHG signal, $\chi^{(2)}_{QW}$ of magnitude 20 ± 8 nm/V and phase $63°\pm34°$ was determined. This measured $|\chi^{(2)}_{QW}|$ is approximately 100 times the value of $\chi^{(2)}_{GaAs}$ (Ref. 18) and is larger than the theoretical peak of 12 nm/V. Further reductions in the uncertainty in l_c and SHG signal baseline would significantly improve the accuracy in the phase and magnitude. Since the line shapes are not perfect Lorentzians, differences between theory and measurement may arise. Inaccuracies in the measured 1–3 intersubband energy and linewidth, local field effects, and inaccuracies in the theoretical z_{23} may also contribute to the inaccuracy in the theoretical estimate for $\chi^{(2)}_{QW}$.

In conclusion, we have demonstrated intersubband absorption in asymmetric coupled $In_{0.6}Ga_{0.4}As/AlAs$ QWs at 4.1 and 2.1 μm wavelengths, among the shortest wavelength intersubband absorption to date. The measured absorption peak energies are within 10% of the theoretical values. We have also demonstrated SHG of 2.0 μm light using these QWs. This is the shortest wavelength SHG to date in any n-type QW system. Using a FEL tuned to 4.0 μm wavelength as the pump source, a $\chi^{(2)}$ of magnitude 20 ± 8 nm/V, approximately 100 times that of bulk GaAs, is measured. Future SHG measurements at different wavelengths should help to determine the dispersion of $\chi^{(2)}_{QW}$ so that a more rigorous comparison to theory can be made. With these short wavelength intersubband transitions, InGaAs/AlGaAs QWs should be useful for nonlinear optical frequency conversion using diode laser sources near 2 μm.

H. C. Chui acknowledges fellowship support from the Office of Naval Research (ONR) and Center for Nonlinear Optical Materials (CNOM), E. L. Martinet, from ONR and Lockheed, and G. L. Woods, from CNOM. This work was supported by ONR under Contract No. N00014-91-C-0170 and Contract No. N00014-92-J-1903, by ARPA under Contract No. N00014-90-J-4056, and CNOM under Contract No. N00014-92-J-1903. FTIR measurements were performed on a Bruker FTIR at the Stanford Free Electron Laser facility.

[1] M. M. Fejer, S. J. B. Yoo, R. L. Byer, A. Harwit, and J. S. Harris, Jr., Phys. Rev. Lett. **62**, 1041 (1989).
[2] E. Rosencher, P. Bois, J. Nagle, and S. Delaitre, Electron. Lett. **25**, 1041 (1989).
[3] S. J. B. Yoo, M. M. Fejer, R. L. Byer, and J. S. Harris, Jr., Appl. Phys. Lett. **58**, 1724 (1991).
[4] C. Sirtori, F. Capasso, D. L. Sivco, S. N. G. Chu, and A. Y. Cho, Appl. Phys. Lett. **59**, 2302 (1991).
[5] J. Khurgin, J. Opt. Soc. Am. B **6**, 1673 (1989).
[6] Y. Hirayama, J. H. Smet, L. H. Peng, C. G. Fonstad, and E. P. Ippen, Appl. Phys. Lett. **63**, 1663 (1993).
[7] H. C. Chui, E. L. Martinet, M. M. Fejer, and J. S. Harris, Jr., Appl. Phys. Lett. **64**, 736 (1994).
[8] H. K. Choi, S. J. Eglash, and M. K. Connors, Appl. Phys. Lett. **63**, 3271 (1993).
[9] E. L. Martinet, G. L. Woods, H. C. Chui, J. S. Harris, Jr., M. M. Fejer, C. A. Rella, and B. A. Richman, in SPIE Proceedings: Quantum Well and Superlattice Physics V (1994), Vol. 2139.
[10] H. C. Chui and J. S. Harris, Jr., J. Vac. Sci. Technol. B **12**, 1019 (1994).
[11] S. M. Lord, B. Pezeshki, and J. S. Harris, Jr., Electron. Lett. **28**, 1193 (1992).
[12] H. C. Chui, S. M. Lord, E. Martinet, M. M. Fejer, and J. S. Harris, Jr., Appl. Phys. Lett. **63**, 364 (1993).
[13] L. C. West and S. J. Eglash, Appl. Phys. Lett. **46**, 1156 (1985).
[14] Y. R. Shen, *The Principles of Nonlinear Optics* (Wiley, New York, 1984).
[15] T. I. Smith, H. A. Schwettman, K. W. Berryman, and R. L. Swent, in SPIE Proceedings: Free Electrons Laser Spectroscopy in Biology, Medicine, and Material Science, edited by H. A. Schwettman, 1993, Vol. 1854, pp. 23–33.
[16] A. N. Pikhtin and A. D. Yas'kov, Sov. Phys. Semicond. **12**, 622 (1978).
[17] S. K. Kurtz, in *Quantum Electronics Volume I: Nonlinear Optics, Part A*, edited by H. Rabin and C. L. Tang (Academic, New York, 1975), pp. 209–281.
[18] B. F. Levine and C. G. Bethea, Appl. Phys. Lett. **20**, 272 (1972).

Tunable mid-infrared generation by difference frequency mixing of diode laser wavelengths in intersubband InGaAs/AlAs quantum wells

H. C. Chui,[a] G. L. Woods, M. M. Fejer, E. L. Martinet,[b] and J. S. Harris, Jr.
Center for Nonlinear Optical Materials, McCullough 226, Stanford University, Stanford, California 94305-4055

(Received 16 June 1994; accepted for publication 10 November 1994)

We demonstrate difference frequency generation (DFG) of 8.66–11.34 μm wavelength light in intersubband InGaAs/AlAs quantum wells by mixing of 1.92 μm±25 nm and 2.39 μm±39 nm. The peak DFG second order nonlinear susceptibility $\chi^{(2)}$ is measured to be 12±1 nm/V, more than 65 times that of GaAs, at a difference frequency output wavelength of 9.50 μm. The intersubband absorption for the 1–2 and 1–3 transitions is measured to be 9.3 and 2.1 μm, respectively. Second harmonic generation (SHG) of 4.76, 5.12, and 5.36 μm light with a CO_2 laser is observed with a peak SHG $\chi^{(2)}$ of 52±3 nm/V. Good agreement of experiment with theory is found for both the linear and nonlinear optical properties. This demonstration of mid-infrared DFG opens the possibility for monolithic diode laser pumps and compact waveguide frequency converters as tunable midinfrared sources. © *1995 American Institute of Physics.*

Compact mid-infrared sources have many potential applications from pollution monitoring and intelligent process controls to laser radar and noninvasive medical diagnosis. Recent developments in long wavelength diode lasers have pushed room temperature continuous operation to 2.3 μm using GaSb based materials.[1,2] However, room temperature operation of diode lasers of wavelengths much longer than 4 μm may not be possible due to Auger recombination.[3,4] In particular, the 8–12 μm atmospheric window may not be attainable at all with such lasers. An alternative approach is to use frequency conversion of near-infrared diode lasers to generate mid-infrared light. Intersubband quantum wells (QWs) are promising materials for such frequency conversion processes. Intersubband QWs have been demonstrated to have nonlinear susceptibilities several orders of magnitude larger than bulk materials.[5–8] Another important advantage of using QWs is the possibility of fabricating monolithic diode laser pumps and quasi-phasematched QW frequency converters as compact mid-infrared sources. Previously, these intersubband transitions had been limited to the far and mid-infrared, but recent advances in strained QW materials have allowed intersubband nonlinearities to reach near-infrared wavelengths[9–12] so that diode lasers could be used to pump the frequency conversion processes.

In this letter, we use the high indium content InGaAs/AlAs QW system which yields short wavelength intersubband transitions due to the large available conduction band offsets. First, the linear spectroscopy of the intersubband transitions will be discussed, followed by second harmonic generation (SHG) characterization of the QW second order nonlinear susceptibility $\chi^{(2)}$. Finally difference frequency generation (DFG) is demonstrated by mixing of near-infrared wavelengths of light to cover most of the 8–12 μm band.

The QW sample used for these studies was designed for mixing of wavelengths around 2 μm to generate 10 μm light. The sample was composed of 300 coupled QWs separated by 50 Å AlAs barriers. The coupled QWs consisted of $In_{0.5}Ga_{0.5}As$ wells of 9 and 7 monolayers in width separated by a 3 monolayer AlAs barrier. One monolayer of GaAs was added to either side of the coupled QW for interface smoothing.[13] The QWs were doped uniformly across the well regions at 5.0×10^{18} cm^{-3} for a sheet charge density of 2.3×10^{12} cm^{-2} per QW. The sample was grown on a (100) semi-insulating GaAs substrate by molecular beam epitaxy (MBE) in a Varian Gen II system with As_2 at a substrate temperature of 360 °C (calibrated by band edge absorption). A linearly graded InGaAs buffer with a final indium composition of 30% was used for strain compensation.[13,14]

The intersubband transition energies were calculated using a single band effective mass model with nonparabolicity included.[12] The transitions were predicted to be $E_{12}=107$ meV (11.6 μm) and $E_{13}=546$ meV (2.27 μm) with dipole moments of $z_{12}=12.3$ Å, $z_{13}=-5.8$ A, and $z_{23}=7.5$ Å. A Fourier transform infrared radiation (FTIR) spectrometer was used to measured the absorption from the sample. The measurement was performed with the sample mounted at Brewster's angle to TM polarized light. The measured absorption spectrum is shown in Fig. 1. Absorption peaks of $E_{12}=133$ meV (9.3 μm) and $E_{13}=591$ meV (2.10 μm) were observed. This E_{13} is one of the largest 1–3 transition energies to date.[9] The half-width at half-maximum (HWHM) transition linewidths were $\Gamma_{12}=11.5$ meV and $\Gamma_{13}=41.6$ meV. Assuming $z_{12}=12.3$ Å from theory, an effective sheet charge density of $\sigma_{\text{eff}}=4.7\times10^{11}$ cm^{-2} per double QW was extracted.[15]

The second order nonlinear susceptibility $\chi^{(2)}$ of the QWs was calculated using a simple perturbative model[16] with linewidths and effective carrier concentration taken from the absorption measurement and dipole moments from theory.[9,17] For SHG, the calculated $\chi^{(2)}$ is plotted in Fig. 2. The two peaks in the QW $\chi^{(2)}$ at 9.55 and 4.3 μm correspond to singly resonant conditions, where the pump photon energy matches E_{12} and the second harmonic photon energy

[a]Present address: Semiconductor Materials Division, Sandia National Laboratories, P. O. Box 5800, Mail Slot 0603, Albuquerque, NM 87185-0603.
[b]Present address: Institute for Micro & Optoelectronics, Ecole Polytechnique Federale de Lausanne, Department of Physics, CH-1015 Lausanne, Switzerland.

 0003-6951/95/66(3)/265/3/$6.00

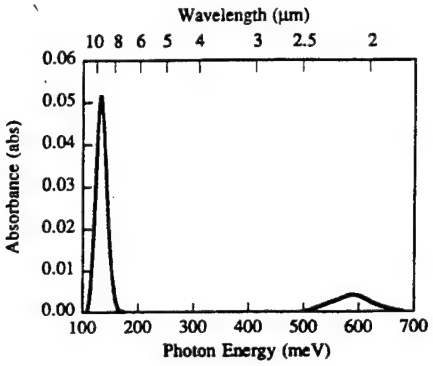

FIG. 1. Intersubband absorption spectrum of the asymmetric coupled QW sample showing peaks at 9.3 and 2.1 μm corresponding to the 1–2 and 1–3 transitions.

matches E_{13}, respectively. An interferometric technique was used to measure the QW $\chi^{(2)}$.[9,17] The SHG from the sample is a superposition of the fields from the GaAs substrate and QW. The $\chi^{(2)}$ tensor elements for the GaAs (xyz) and QW (zzz) are different so that polarization selection can be used to extract only the QW contribution. By selecting only TM polarizations, this extraction can be performed by measuring the SHG from the sample versus azimuthal angle ϕ of the sample about its normal (ϕ scans). With only a GaAs contribution, the SHG power is fourfold symmetric about the (001) normal to the sample. By adding a QW contribution, the SHG power becomes only twofold symmetric.[9]

The SHG measurements were performed with a CO_2 laser tuned to pump wavelengths of 9.51, 10.23, and 10.72 μm. The CO_2 laser used for the experiment generated ~300 ns pulses with peak powers of ~1 kW. The pump beam was focused down to a ~100 μm diameter spot on the sample. A multilayer dielectric filter was placed before the sample to block light at wavelengths shorter than ~8 μm. An InSb detector was used to measure the SHG power, and ZnSe polarizers were used to select only the TM polarization. A fraction of the pump was focused onto a $AgGaSe_2$ crystal as a reference SHG signal. Normalization of the SHG signal from the sample to fluctuations in the pump power were then eliminated by ratioing the SHG signal to the reference SHG power. Although we did not calibrate the setup for absolute

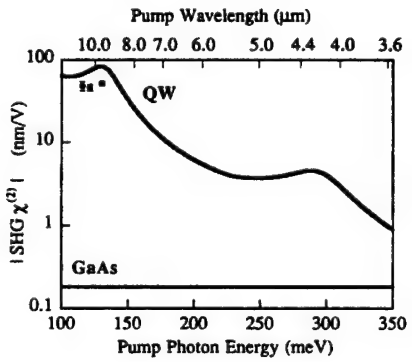

FIG. 2. Measured (points) and theoretical (solid curve) SHG $\chi^{(2)}$.

power measurements, we estimate that the peak SHG power from the sample was on the order of a few milliwatts. With this setup, ϕ scans were taken at an incidence angle of ~45°. The parameters for extracting the QW $\chi^{(2)}$ were sample thickness of 384±1 μm, total MQW thickness of 3.3 μm, and bulk coherence lengths of 108.9±1, 107.5±1, and 105.6±1 μm at 9.51, 10.23, and 10.72 μm, respectively. The coherence lengths were calculated from published refractive index data.[18] The resulting measured QW $\chi^{(2)}$ values for SHG are shown in Fig. 2. The maximum QW $\chi^{(2)}$ of 52±3 nm/V, 280 times the bulk GaAs $\chi^{(2)}$ of 180 pm/V,[19] was measured at a pump wavelength of 9.51 μm. The error bars are absolute errors in the measured values resulting from inaccuracies in the sample thickness and coherence lengths. Good agreement of these measured values to theory is observed with slight deviations arising from inaccuracies in the coherence lengths, sample thickness, or transition line shapes.

DFG measurements were performed using the same interferometric technique. The two pump beams for the DFG experiment were taken from an optical parametric oscillator (OPO). This OPO consisted of two walk-off compensated KTP crystals pumped by a Nd:YAG laser at a wavelength of 1.064 μm. Thus, the OPO signal and idler output beams have photon energies which sum to a 1.064 μm photon energy. The OPO used for this experiment generated pulses of ~10 ns duration with peak powers of several hundred kilowatts. Tuning of the OPO was accomplished by adjusting the angle of the KTP crystals, and a spectrometer with an InSb detector was used to accurately determine both of the pump wavelengths. Two 1.064 μm high reflectors were used to eliminate any transmitted 1.064 μm light, and a rutile prism polarizer was used to select the TM polarization for both beams to the sample. Glass filters were placed before the sample to eliminate any light at wavelengths longer than ~3 μm. A HgCdTe detector with a Ge window was used to measure the DFG signal. Several multilayer dielectric filters were used and verified to eliminate any radiation at wavelengths shorter than ~8 μm while the HgCdTe detector response ensured that radiation at wavelengths longer than ~12 μm was not detected. A wire grid polarizer was used to select only the TM polarization of the DFG output.

For DFG output wavelengths between 8 and 12 μm, the coherence length in GaAs is fairly short, on the order of 30 μm as calculated from refractive index data. Since the sample thickness is 384±1 μm, small inaccuracies in the coherence length cause large inaccuracies in the GaAs contribution to the DFG. This inaccuracy can be eliminated by determining the wavelength at which the GaAs contribution is null; this was accomplished by minimizing the DFG power while tuning the OPO. Using the technique, a GaAs null was measured at a DFG output wavelength of 8.86±0.05 μm. If the coherence lengths calculated from refractive index data are assumed to be correct, an effective sample length of 376.6±1.5 μm yields the correct GaAs null wavelength. On opposite sides of this GaAs null wavelength, the GaAs contribution to the DFG field has opposite signs; ϕ scans at 8.66 and 9.00 μm showing DFG power versus sample azimuthal angle are plotted in Fig. 3. The asymmetry between the 0°

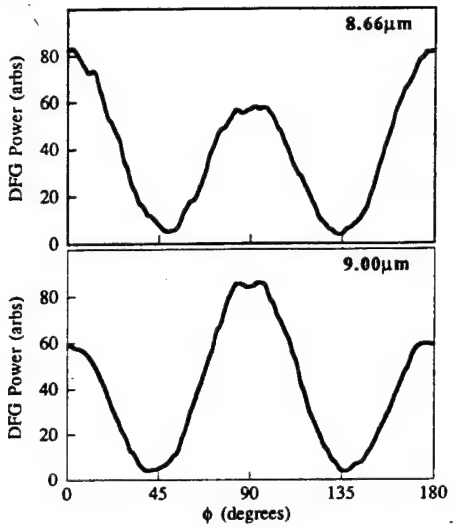

FIG. 3. DFG power vs azimuthal angle ϕ of the sample at output wavelengths of 8.66 and 9.00 μm showing opposite signs of asymmetry due to a sign reversal of the bulk GaAs contribution.

(or 180°) and 90° (or 270°) peaks arises from a QW contribution to the DFG signal. The opposite signs in the GaAs contribution for the two wavelengths result in opposite signs in the asymmetry in the peaks; at 8.66 μm, the 0° peak is higher than the 90° peak, while at 9.00 μm, the 90° peak is higher than the 0° peak.

By taking ϕ scans and using the calculated coherence lengths and effective sample length, accurate determination of the QW DFG $\chi^{(2)}$ was obtained over a wide wavelength range in the 8–12 μm window. A plot of the measured QW DFG $\chi^{(2)}$ versus DFG output wavelength is shown in Fig. 4. The error bars were determined from inaccuracy in the measured effective sample length. The theoretical DFG $\chi^{(2)}$ for this process was calculated using the same parameters (dipole moments, linewidths, and effective carrier concentration) in the same perturbative expression[16] as was used for the SHG $\chi^{(2)}$. This theoretical DFG $\chi^{(2)}$ is also plotted in Fig. 4. Excellent agreement of experiment to theory is observed. A peak DFG $\chi^{(2)}$ of 12±1 nm/V, more than 65 times that of bulk GaAs (also 180 pm/V for these wavelengths as calculated using Miller's rule),[19] at an output wavelength of 9.50 μm is measured. Tunable radiation from 8.66 to 11.34 μm was generated with large $\chi^{(2)}$'s for only slight tuning of the pump wavelengths (1.92 μm±25 nm and 2.39 μm±39 nm). This is the first demonstration of mid-infrared DFG in any QW system; far-infrared DFG by mixing of two CO_2 lasers in intersubband QWs was recently demonstrated.[20] The pump wavelengths used for our DFG coincide with recent room temperature diode laser wavelengths[1] so that integration of such a mixer with diode lasers might be possible.

In conclusion, we have demonstrated DFG of mid-infrared light by mixing of diode laser wavelengths in intersubband InGaAs/AlAs QWs. We have characterized the linear absorption and nonlinear optical properties; SHG and DFG were used to measure the $\chi^{(2)}$ of the QWs. Both measured absorption and $\chi^{(2)}$ are found to be in good agreement with theory. With large nonlinearities at diode laser wavelengths, these intersubband QWs combined with diode laser pumps should result in efficient difference frequency mixers as compact mid-infrared sources operating at room temperature.

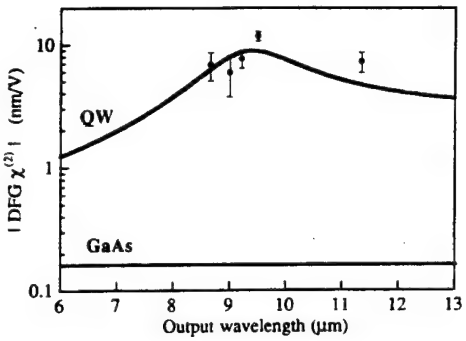

FIG. 4. Measured (points) and theoretical (solid curve) DFG $\chi^{(2)}$ for mixing of the signal and idler outputs from a 1.064 μm pumped OPO.

One of us (H.C.C.) acknowledges fellowship support from the Office of Naval Research (ONR) and Center for Nonlinear Optical Materials (CNOM), E. L. Martinet, from ONR and Lockheed, and G. L. Woods, from CNOM. This work was supported by ONR under Contract No. N00014-91-C-0170 and Contract No. N00014-92-J-1903, by ARPA under Contract No. N00014-90-J-4056, and CNOM under Contract No. N00014-J-1903. FTIR measurements were performed on a Bruker FTIR at the Stanford Free Electron Laser facility. The DFG measurements were performed at Lightwave Electronics where W. R. Bosenberg generously provided us time on his OPO.

[1] S. J. Eglash and H. K. Choi, Appl. Phys. Lett. **57**, 1292 (1990).
[2] H. K. Choi and S. J. Eglash, Appl. Phys. Lett. **61**, 1154 (1992).
[3] S. J. Eglash and H. K. Choi, Appl. Phys. Lett. **64**, 833 (1994).
[4] S. R. Kurtz, R. M. Biefeld, L. R. Dawson, K. C. Baucom, and A. J. Howard, Appl. Phys. Lett. **64**, 812 (1994).
[5] M. M. Fejer, S. J. B. Yoo, R. L Byer, A. Harwit, and J. S. Harris, Jr., Phys. Rev. Lett. **62**, 1041 (1989).
[6] E. Rosencher, P. Bois, J. Nagle, and S. Delaitre, Electron. Lett. **25**, 1041 (1989).
[7] S. J. B. Yoo, M. M. Fejer, R. L. Byer, and J. S. Harris, Jr., Appl. Phys. Lett. **58**, 1724 (1991).
[8] C. Sirtori, F. Capasso, D. L. Sivco, S. N. G. Chu, and A. Y. Cho, Appl. Phys. Lett. **59**, 2302 (1991).
[9] H. C. Chui, E. L. Martinet, G. L. Woods, M. M. Fejer, J. S. Harris, Jr., C. A. Rella, B. I. Richman, and H. A. Schwettman, Appl. Phys. Lett. **64**, 3365 (1994).
[10] E. L. Martinet, H. C. Chui, G. L. Woods, M. M. Fejer, J. S. Harris, Jr., C. A. Rella, B. I. Richman, and H. A. Schwettman, Appl. Phys. Lett. **65**, 2630 (1994).
[11] Y. Hirayama, J. H. Smet, L. H. Peng, C. G. Fonstad, and E. P. Ippen, Appl. Phys. Lett. **63**, 1663 (1993).
[12] H. C. Chui, E. L. Martinet, M. M. Fejer, and J. S. Harris, Jr., Appl. Phys. Lett. **64**, 736 (1994).
[13] H. C. Chui and J. S. Harris, Jr., J. Vac. Sci. Technol. B **12**, 1019 (1994).
[14] S. M. Lord, B. Pezeshki, andJ. S. Harris, Jr., Electron. Lett. **28**, 1193 (1992).
[15] L. C. West and S. J. Eglash, Appl. Phys. Lett. **46**, 1156 (1985).
[16] Y. R. Shen, *The Principles of Nonlinear Optics* (Wiley, New York, 1984).
[17] E. L. Martinet, G. L. Woods, H. C. Chui, J. S. Harris, Jr., M. M. Fejer, C. A. Rella, and B. I. Richman, in *Quantum Well and Superlattice Physics V* (SPIE, Bellingham, WA, 1994), Vol. 2139, p. 331.
[18] A. N. Pikhtin and A. D. Yas'kov, Sov. Phys. Semicond. **12**, 622 (1978).
[19] B. F. Levine and C. G. Bethea, Appl. Phys. Lett. **20**, 272 (1972).
[20] C. Sirtori, F. Capasso, J. Faist, L. N. Pfeiffer, and K. W. West, Appl. Phys. Lett. **65**, 445 (1994).

Intersubband transitions in high indium content InGaAs/AlGaAs quantum wells

H. C. Chui, S. M. Lord, E. Martinet, M. M. Fejer, and J. S. Harris , Jr.
Center for Nonlinear Optical Materials, Stanford University, Stanford, California 94305-4055

(Received 8 March 1993; accepted for publication 17 May 1993)

We report the first observation of intersubband transitions in $In_yGa_{1-y}As(y=0.3,0.5)$/AlGaAs quantum wells. These quantum wells were grown on a GaAs substrate with a linearly graded InGaAs buffer to achieve strain relaxation before growth of the quantum wells. Measured intersubband transition energies of 316 and 350 meV are among the largest ever reported. Asymmetric step $In_{0.5}Ga_{0.5}As$/AlGaAs quantum wells designed for second harmonic generation measurements also demonstrate strong intersubband absorption at 224 meV corresponding to the 1-2 transition. With the large conduction band offsets (larger than 800 meV) available in this material system, extension to larger intersubband transitions energies for quantum well photodetector and nonlinear optics applications should be possible.

Large intersubband transition energies are essential for extending the operating wavelength of quantum well infrared photodetectors (QWIPs) and intersubband nonlinear optical frequency conversion devices.[1] QWIPs have recently been a topic of interest for applications in high speed detector arrays.[2] By using large energy intersubband transitions in quantum wells, the useful range of these QWIPs can be extended to the 3–5 μm atmospheric window. Also of interest is the application of large intersubband transition energies to nonlinear optical frequency conversion devices. With the demonstration of large nonlinear optical susceptibilities in quantum wells,[3] large intersubband transition energies would similarly extend the range of available frequencies for nonlinear interactions. Large intersubband transition energies have been observed in quantum wells of GaAs/AlAs (E_{16}=434 meV)[4] on GaAs as well as InGaAs/InAlAs on InP (E_{12}=400 meV for strained quantum wells and E_{12}=295 meV for lattice matched).[5–7] By using InGaAs/AlGaAs quantum wells, the conduction band offset ΔE_c is further extended. However, the lattice mismatch of InGaAs and AlGaAs limits the range of useful indium content for producing good quality material. Thus, prior to this work, intersubband transitions had only been observed in InGaAs/AlGaAs quantum wells of up to 15% indium concentration.[8] By using a linearly compositionally graded buffer, Lord *et al.*[9] demonstrated that high quality $In_{0.5}Ga_{0.5}As$/AlGaAs quantum wells could be grown on a GaAs substrate. Using this novel growth technique, we investigate intersubband transitions in InGaAs/AlGaAs quantum wells with high indium concentrations of 30% and 50%. We first present results on intersubband transitions in two square well samples before reporting on an asymmetric step multiple quantum well designed for future intersubband second harmonic generation measurements.

Two $In_yGa_{1-y}As/Al_{0.45}Ga_{0.55}As$ square multiple quantum well (MQW) samples were grown with well indium compositions of y=0.3 and 0.5. The targeted layer structures for these samples are shown in Fig. 1. These MQW structures were grown on semi-insulating GaAs substrates by molecular beam epitaxy (MBE) in a Varian Gen-II system using As_2 at a substrate temperature of 480 °C. The MQWs were grown atop an InGaAs buffer which was linearly graded at a rate of 16% indium/μm from GaAs to approximately the average indium composition of the MQWs. The indium compositions of the wells were measured by performing x-ray diffraction (XRD) on two thick, relaxed InGaAs samples grown in the same growth run and with the same growth rates as the MQW samples. The actual well compositions were determined to be y=0.28 and 0.51. The samples were doped n^+ in the well regions with measured Hall sheet charge densities per quantum well of $n=2.56\times10^{12}$ and 5.56×10^{12} cm^{-2} for the y=0.3 and 0.5 samples, respectively.

The intersubband absorption was measured using a Fourier transform infrared spectrometer (FTIR) with the samples mounted at the Brewster angle to the TM polarized light. The FTIR spectra for the two square MQW samples are shown in Fig. 2. The measured absorption peaks for the 1-2 transitions were found to be 316 and 350 meV with full width at half-maximum (FWHM) linewidths of 37.5 and 52.9 meV for the y=0.3 and 0.5 samples, respectively. These intersubband transition energies are among the largest ever reported and are comparable to the theoretically calculated values of 330 meV for both the y=0.3 and y=0.5 samples. These values were calculated using a single band effective mass model[10] with nonpara-

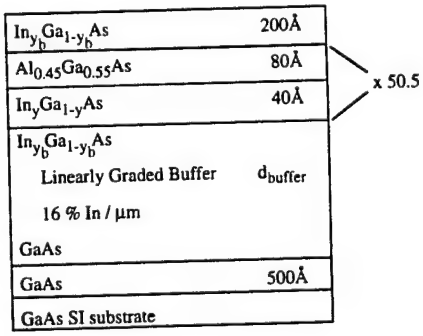

FIG. 1. Layer structure for $In_yGa_{1-y}As$/AlGaAs square MQWs with graded InGaAs buffer for (a) y=0.3 sample: y_b=0.11, d_{buffer} = 6000Å and (b) y=0.5 sample: y_b=0.17, d_{buffer}=10 000 Å.

 0003-6951/93/63(3)/364/3/$6.00

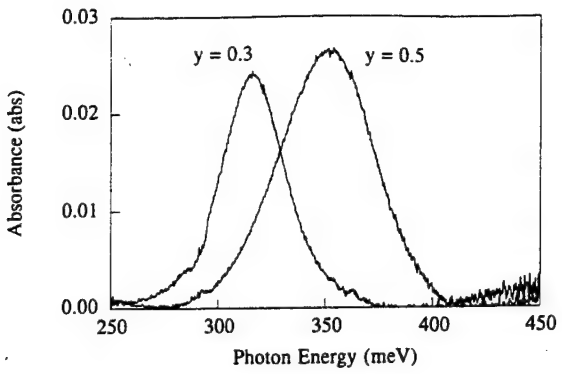

FIG. 2. FTIR absorption spectra of the $y=0.3$ and 0.5 square MQW samples.

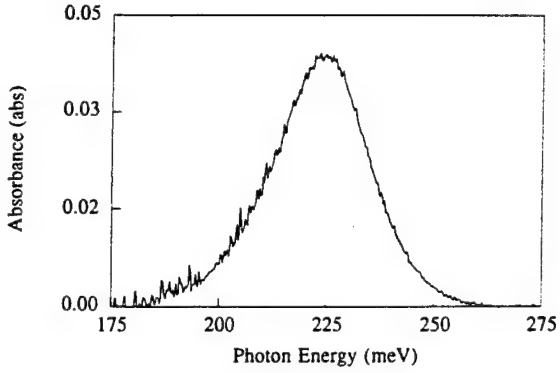

FIG. 4. FTIR absorption spectrum of the InGaAs/AlGaAs asymmetric step MQW sample.

bolicity included via an energy dependent effective mass derived from the conduction band dispersion. The calculated values for the two composition wells are approximately the same because the change in well depth is offset by differences in the effective mass and band nonparabolicity. The measured integrated absorption fractions, IAFs, were found to be 0.965 abs-meV and 1.489 abs-meV resulting in dipole moments[11] of 8.3 and 7.0 Å for the $y=0.3$ and 0.5 samples, respectively. The theoretically calculated dipole moments using the measured sheet charge densities are 12 Å for both samples.

An asymmetric step quantum well sample was also grown for future second harmonic generation measurements.[12,13] This sample, however, was grown using As_4 at a substrate temperature of 430 °C. The conduction band diagram for the asymmetric step quantum wells of this sample with theoretically calculated energy levels is shown in Fig. 3. This sample was doped n^+ in the 40 Å well regions only, resulting in a measured Hall sheet charge density of 2.94×10^{12} cm^{-2} per quantum well. The structure was similar to that shown in Fig. 1. However, the final buffer composition y_b was 0.19, and the buffer was graded at a rate of 8% indium/μm to further improve the material quality in the MQW region.[14] High resolution XRD measurements of a reference wafer grown in the same growth run and with thick relaxed InGaAs layers corresponding to the buffer and well determined that the actual well, step, and buffer compositions were 0.54, 0.24, and 0.20, respectively, instead of the targeted 0.47, 0.23, and 0.19.

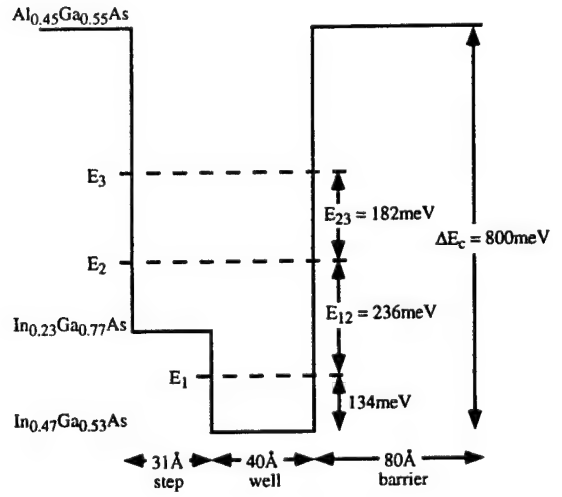

FIG. 3. Conduction band diagram of asymmetric step MQW sample with theoretically calculated energy levels

The absorption spectrum of the asymmetric step MQW sample was measured using FTIR, and the spectrum is plotted in Fig. 4. A strong intersubband absorption at 224 meV with a FWHM of 27 meV corresponding to the 1-2 transition is observed. The transition energy is close to the theoretically calculated value of 236 meV. The measured IAF is 1.26 abs-meV resulting in a dipole moment of 10.4 Å for this transition. This dipole moment is different from the calculated value of 15 Å.

In summary, we report the first observation of intersubband transitions in high indium content InGaAs/AlGaAs square and asymmetric step quantum wells. The intersubband transition energies of 316 and 350 meV measured for the $y=0.3$ and 0.5 square well samples, respectively, are among the largest ever reported. Intersubband absorption at 224 meV was also observed in an asymmetric step quantum well sample. The key element to the successful growth was the use of a linearly graded InGaAs buffer. Thus we have demonstrated that the strained InGaAs/AlGaAs system grown on a linearly graded InGaAs buffer is a material system that should prove useful for applications where extremely large conduction band offsets are needed. With the $In_{0.5}Ga_{0.5}As/Al_{0.45}Ga_{0.55}As$ quantum wells, there is a conduction band offset of 800 meV, and by further increasing the indium content in the wells and the aluminum content in the barriers, even larger conduction band offsets and intersubband transition energies are obtainable. Applications such as short wavelength quantum well photodetectors, resonant tunneling diodes, and near infrared intersubband nonlinear optical frequency converters should be possible.

H. C. Chui acknowledges fellowship support from the Office of Naval Research (ONR), E. Martinet, from ONR and Lockheed, and S. M. Lord, from AT&T. This work was supported by ONR under Contract Nos. N00014-91-J-0170 and N00014-92-J-1903 and by DARPA under Contract No. N00014-90-J-4056.

[1] *Intersubband Transitions in Quantum Wells*, edited by E. Rosencher, B. Vinter, and B. Levine (Plenum, New York, 1992).
[2] C. G. Bethea, B. F. Levine, V. O. Shen, R. R. Abbott, and S. J. Hseih, IEEE Electron Devices. **38**, 1118 (1991).
[3] M. M. Fejer, S. J. B. Yoo, R. L. Byer, A. Harwit, and J. S. Harris, Jr., Phys. Rev. Lett. **62**, 1041 (1989).
[4] J. L. Pan, L. C. West, S. J. Walker, R. J. Malik, and J. F. Walker, Appl. Phys. Lett. **57**, 366 (1990).
[5] H. Asai and Y. Kawamura, Appl. Phys. Lett. **56**, 746 (1990).
[6] B. F. Levine, A. Y. Cho, J. Walker, R. J. Malik, D. A. Kleinman, and D. L. Sivco, Appl. Phys. Lett. **52**, 1481 (1988).
[7] S. D. Gunapala, B. F. Levine, D. Ritter, R. Hamm, and M. B. Panish, J. Appl. Phys. **71**, 2458 (1992).
[8] X. Zhou, P. K. Bhattacharya, G. Hugo, S. C. Hong, and E. Gulari, Appl. Phys. Lett. **54**, 855 (1989).
[9] S. M. Lord, B. Pezeshki, and J. S. Harris, Jr., Electron. Lett. **28**, 1193 (1992).
[10] G. Bastard, *Wave Mechanics Applied to Semiconductor Heterostructures* (Les Èditions de Physique, France, 1988), Chap. 2.
[11] L. C. West and S. J. Eglash, Appl. Phys. Lett. **46**, 1156 (1985).
[12] S. J. B. Yoo, M. M. Fejer, R. L. Byer, and J. S. Harris, Jr., Appl. Phys. Lett. **58**, 1724 (1991).
[13] P. Boucaud, F. H. Julien, D. D. Yang, J-M. Lourtioz, E. Rosencher, P. Bois, and J. Nagle, Appl. Phys. Lett. **57**, 215 (1990).
[14] S. M. Lord, B. Pezeshki, A. F. Marshall, J. S. Harris, Jr., R. Fernandez, and A. Harwit, Materials Research Society Fall Meeting, 1992, Symposium D, Paper No. D2.7.

Fabrication of GaAs Orientation Template Substrates for Quasi-Phasematched Guided-Wave Nonlinear Optics

L.A. Eyres, C.B. Ebert, J.S. Harris, Jr. and M.M. Fejer
Center for Nonlinear Optical Materials
E.L. Ginzton Laboratory, Stanford University, Stanford, CA 94305
phone (415) 723-1718: fax (415) 723-2666

H. C. Chui
Org 1311, MS 0603, P.O. Box 5800
Sandia National Laboratories
Albuquerque, NM 87185
phone (505) 844-8735: fax (505) 844-8985

Quasi-phasematched nonlinear optical frequency conversion in waveguides is a flexible and efficient technique for generating visible and infrared radiation from low-power near infrared diode lasers. While demonstrated conversion efficiencies have been high[1-3], a formidable difficulty remains in the path of widespread implementation of waveguide frequency conversion techniques. The separately fabricated diode lasers and nonlinear waveguides must be aligned together to sub-micron tolerances with high yield and excellent long-term reliability. Monolithic integration of diode lasers and nonlinear devices onto the same substrate is an attractive solution to this problem, particularly if the nonlinear devices are fabricated in semiconductor materials.

The zincblende III-V and II-VI semiconductors have large second order nonlinear optical susceptibilities, but because they lack both birefringence and a spontaneous ferroelectric polarization, they can not be birefringently phasematched or quasi-phasematched using ferroelectric domain inversion techniques applied to other material systems. High efficiency quasi-phasematched nonlinear optical devices require long interaction lengths and significant modulation of the nonlinear susceptibility.[4] In semiconductors this modulation can be achieved by a physical reorientation of the crystal axes relative to the propagating radiation. Different schemes have been studied for achieving this, including wafer bonding[5] and patterned epitaxy.[6]

We propose a technique for fabricating quasi-phasematched nonlinear optical waveguides in zincblende semiconductor materials employing a general orientation template substrate in GaAs. Waveguides made up of any of a variety of materials can be grown on this substrate, provided that the waveguiding layers grow with high optical quality and follow the orientation pattern of the template. This approach transforms the obscure problem of achieving the periodic crystal reorientation necessary for QPM into the more familiar problem of heteroepitaxy. The process should be applicable to materials such as II-VI semiconductors and even the wide-bandgap III-Vs for blue and ultraviolet light generation.

Zincblende crystals belong to symmetry group $\bar{4}3m$, which requires $\chi^{(2)}_{xyz}$ to be the only non-zero tensor element of the second-order nonlinear susceptibility. Since a $\bar{4}$ axis lies along <100>, a 90° rotation of the lattice about <100> results in an effective crystalline inversion, reversing the direction of each column III-column V bond and changing the sign of $\chi^{(2)}_{xyz}$ as seen by the radiation. The availability of substrate orientation (100) is fortunate: the 90° rotation about [100] necessary to perform a crystal inversion leaves the same plane exposed for

subsequent growth. This avoids potential problems associated with differences in growth rate on a substrate containing two different crystalline orientations.

An outline of the fabrication process for the template substrate is shown in figure 1. Thin layers of $Al_{0.7}Ga_{0.3}As$ (0.5μm) and GaAs (0.1μm) are grown on a semi-insulating (100) GaAs substrate using molecular beam epitaxy (MBE). The $Al_{0.7}Ga_{0.3}As$ layer serves as an etch stop for subsequent processing, while the GaAs layer provides the seed layer necessary for the modulation of crystal orientation. Wafer pieces of approximately $1cm^2$ are then cleaved from this wafer and from another wafer without epilayers, the native oxides are stripped off, and the two are placed in contact with their relative orientations differing by a 90° rotation about [100] as detailed above. The contacted sample is then placed into a furnace for wafer bonding[7,8] in an N_2/H_2 atmosphere at 830°C for two hours under a pressure of $1kg/cm^2$. The wafer bonding process fuses the two samples together so that they can be cleaved as a single piece, not breaking in the plane of the interface. After bonding, the original MBE substrate is removed by a combination of mechanical lapping and selective chemical etching which stops on the $Al_{0.7}Ga_{0.3}As$ layer. Selectively stripping the $Al_{0.7}Ga_{0.3}As$ leaves a thin GaAs layer of one crystal orientation bonded to a GaAs substrate of a different orientation. Lithography and chemical etching are used to etch a pattern into the bonded GaAs epilayer, exposing the substrate with its 90° rotated crystal orientation. This two-orientation surface then forms a substrate for subsequent growth of thin film layers which have a built-in modulation of crystal orientation and nonlinear susceptibility. After further cleaning, the template substrates are placed back into the MBE chamber for growth of these layers.

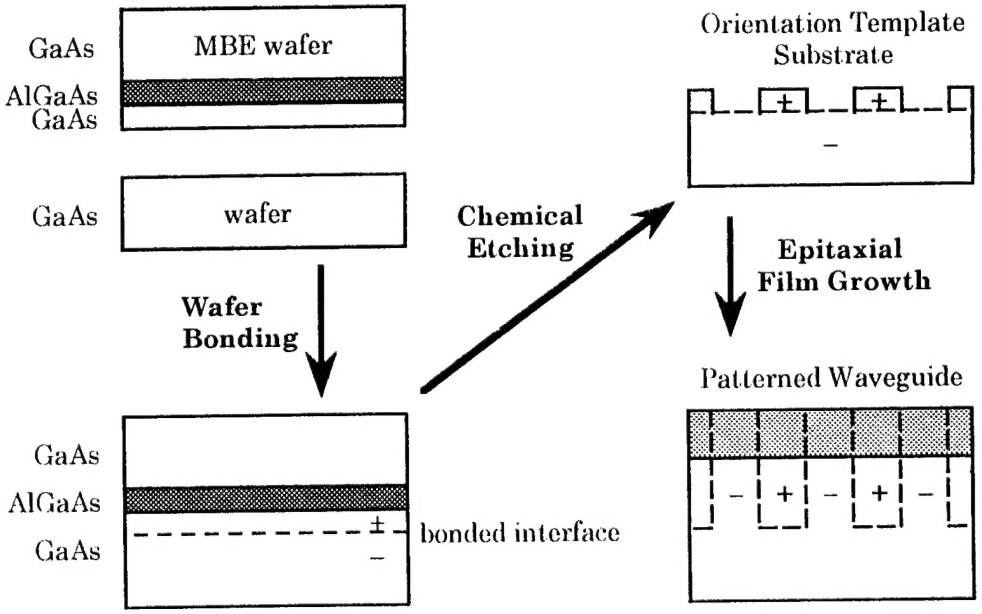

Figure 1: Fabrication process for orientation template substrate and nonlinear grating waveguide. +/- indicates the sign of the nonlinear optical susceptibility as seen by the optical mode.

Figure 2 is a SEM micrograph showing the cleaved cross-section of a thin film (0.5μm GaAs: 0.1μm AlAs: 0.5μm GaAs) grown on a template substrate. The 1500Å deep grating

originally etched into the template substrate to reveal the second orientation is largely preserved during MBE growth, resulting in a surface corrugation of approximately the same magnitude. We observe differences in morphology between gratings oriented along [011] and [$0\bar{1}1$] , which we attribute to differences in growth rates on the sidewall-exposed (111)A and (111)B faces. The cleaved cross sections show no evidence of voids at the grain boundary interfaces under SEM examination.

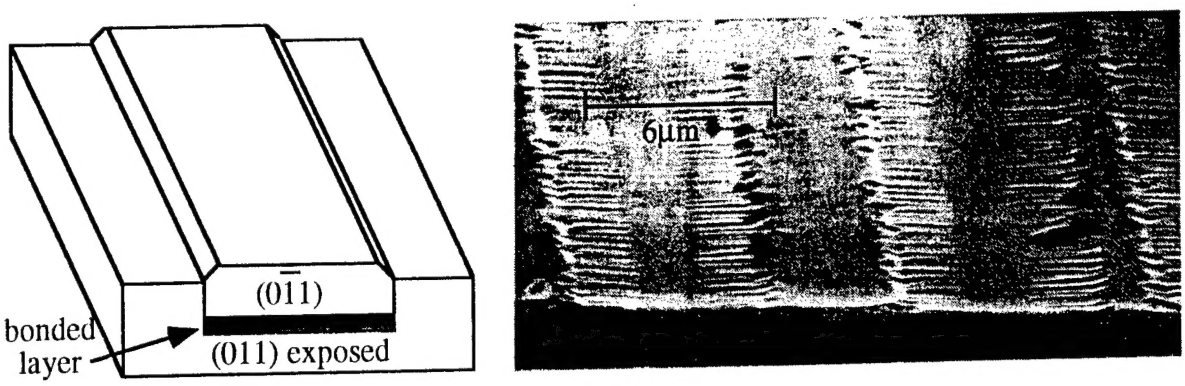

Figure 2: Schematic and SEM micrograph of cleaved cross-section of orientation modulated thin film on orientation template substrate. (0.5μm GaAs: 0.1μm AlAs: 0.5μm GaAs)

X-ray diffraction from {111} planes on these films while rotating the sample about the [100] surface normal reveals that each of the expected four-fold diffraction peaks is made up of two very sharp peaks separated by < 0.5°, confirming that two different high-quality crystalline regions with slight rotational misalignment are present in the near surface region. Angular misalignment of 0.5° is reasonable given the tolerances of our wafer contacting apparatus, Photoluminescence measurements on quantum wells grown on template substrates show strong signals from large regions of each orientation; on short period gratings, the PL signal is significantly reduced, probably due to grain boundary effects. Selective etching experiments have confirmed that the orientation modulation follows the intended pattern down to grating periods as short as 6μm. Additionally, preferential etching at grain boundaries between adjacent regions of the epitaxial film reveals the grain boundaries to be roughly vertical.

We have proposed and demonstrated the growth of GaAs orientation-patterned layers on orientation template substrates. This result opens new avenues for research into semiconductor guided-wave nonlinear devices and their integration with diode lasers.

1 M. Yamada, N. Nada, M. Saitoh, K. Watanabe, Appl. Phys. Lett. **62**, 435 (1993).
2 K. Yamamoto, K. Mizuuchi, Y. Kitaoka, M. Kato, Appl. Phys. Lett. **62**, 2599 (1993).
3 W.P. Risk, W.J. Kozlovsky, S.D. Lau, G.L.Bona, H. Jaeckel, and D.J. Webb, Appl.Phys. Lett. **63**, 3134 (1993).
4 S. Somekh and A. Yariv, Opt. Com., **6**, 301 (1972).
5 L. Gordon, G.L. Woods, R.C. Eckardt, R.R. Route, R.S Feigelson, M.M. Fejer and R.L. Byer, Electronics Letters, **29**, 1942 (1993).
6 M.J. Angell, R.M. Emerson, J.L. Hoyt, J.F. Gibbons, L.A. Eyres, M.L. Bortz, and M.M Fejer, Appl. Phys. Lett. **64**, 3107 (1994).
7 A. Yamada, M. Oasa, H. Nagabuchi and M. Kawashima, Mater. Lett. 6, 167 (1988).
8 Z.L. Liau and D.E. Mull, Appl. Phys. Lett. **56** 737 (1990).